Journal of Computational Physics 228 (2009) 3911–3916

Contents lists available at ScienceDirect

Journal of Computational Physics

journal homepage: www.elsevier.com/locate/jcp

Short Note

The implementation of slide lines as a combined force and velocity boundary condition

E.J. Caramana *

New Paris R.D.#1, Pa., 15554, United States

ARTICLE INFO

Article history:
Received 27 December 2008
Received in revised form 18 February 2009
Accepted 20 February 2009
Available online 6 March 2009

Keywords:
Lagrangian hydrodynamics
Shock waves
Material strength

Slide lines (2D) and surfaces (3D) are a way to treat interfaces in Lagrangian hydrocodes that allow different materials or regions to move relative to each other without the grid distortion that would otherwise terminate these calculations quickly. The Lagrangian frame is natural for Newton's second law of motion, and also for the calculation of the stress deviators of material models. It is not suitable for the computation of fluid instabilities. However, computer codes based in the Lagrangian frame were the first to be developed and the idea of introducing slide lines to avoid premature grid tangling between regions without significant internal vorticity is very old [1]. All slide line treatments have followed this original work of Wilkins, in spirit if not quite in detail, and we herein do the same. Unfortunately slide lines tend to be a very ad-hoc device without a firm theoretical foundation. It is the purpose of this note to clarify the meaning of this construction and to provide a new and more logically cogent implementation.

Slide line treatments consist of two steps: the first is the calculation of forces that act normal to it, but with tangential forces that are discontinuous and thus lead to a discontinuous tangential velocity; however, a discontinuous normal velocity also develops – the so-called "interpenetration" problem. This latter difficulty is fixed by the "put-back-on" step where one declares one side to be the "master" whose positions and velocities are unchanged after the solution of the force equation, and the other as the "slave" whose point positions and normal velocities are made to conform to those of the master. This latter step is not well justified and often leads to unnecessarily complicated interpolations and generally nonrobust and "cludgy" constructs. We begin by briefly deriving the force decomposition step in a simple manner; then, while keeping the master–slave distinction we show how the interpenetration problem is resolved as a proper velocity boundary condition. Finally, total energy balance is considered and a "goodness" criterion for the overall slide line procedure is derived; numerical results are given. What is shown is that slide lines (in 2D or 3D) should be thought of as a special type of velocity boundary condition constructed with respect to a curved surface – the so-called "master" side. However, this master surface is no longer fixed in space as is a solid or reflective boundary. It is also shown how the put-back-on step is related to this new construct and why it has still been useful for so long.

* Tel.: +1 970 493 0554.
E-mail address: ed.caramana@gmail.com

0021-9991/$ - see front matter © 2009 Elsevier Inc. All rights reserved.
doi:10.1016/j.jcp.2009.02.029

We begin with Newton's second law for fluid elements (as opposed to mass points) expressed as:

$$M_p \frac{d\vec{v}_p}{dt} = \vec{F}_p, \tag{0.1}$$

where M_p is the mass associated with a point "p", its velocity is $\vec{v}_p$, and the total force $\vec{F}_p$ acts on it from the surrounding zones "z" due to the stress in these zones; the convective form of the time derivative denotes the Lagrangian frame of reference. We utilize a staggered-spatial-grid with zonal masses M_z and stresses defined in zones, and with point positions, velocities, and masses [2]. This interleaving of spatial variables avoids the well known grid-decoupling, or odd-even, instability that occurs with Lagrangian point-centered schemes even in 1D, and also leads to a very simple way to calculate the force $\vec{F}_p$ acting on a given point from its neighboring zones in multi-dimensions.

The force decomposition step begins by formally dividing Eq. (0.1) for a single point "p" into upper "u" and lower "l" portions as

$$M_{l,p} \frac{d\vec{v}_p}{dt} = \vec{F}_{l,p} + \vec{g}_{l,p}; \quad M_{u,p} \frac{d\vec{v}_p}{dt} = \vec{F}_{u,p} + \vec{g}_{u,p}, \tag{0.2}$$

where the $\vec{g}$'s are the respective contact forces. In order for the above two equations to sum to Eq. (0.1) we require $M_p = M_{l,p} + M_{u,p}$, $\vec{F}_p = \vec{F}_{l,p} + \vec{F}_{u,p}$, and $\vec{g}_{l,p} = -\vec{g}_{u,p}$. That their acceleration be equal to that of the undivided momentum equation yields

$$\vec{g}_{l,p} = -\vec{g}_{u,p} = \frac{M_{l,p}\vec{F}_{u,p} - M_{u,p}\vec{F}_{l,p}}{(M_{l,p} + M_{u,p})}. \tag{0.3}$$

Note about this decomposition: momentum is conserved and the work performed by the net contact forces is zero; this is thus also true in any direction $\hat{c}$. The slide approximation is obtained by first defining unit vectors $\hat{c}_{u,p}$ and $\hat{c}_{l,p}$ at all points "p" of a slide line. Here $\hat{c}_p$ is defined by summing the outward grid vectors adjacent to each point on its respective side and dividing by their magnitude. (For problems involving a special symmetry other choices are possible; for instance, fitting a circle through a point and its two neighbors in 2D or spheres in 3D.) One then lets $\vec{g}_{l,p} \to (\vec{g}_{l,p} \cdot \hat{c}_{l,p})\hat{c}_{l,p}$ in the first part of Eq. (0.2) and likewise ("l" goes to "u") in the second part. (We hereon favor writing formulas for the "l" side; "u" side formulas are obtained simply by switching both "l" and "u".) If Eqs. (0.2) is written normal and tangential to the respective $\hat{c}_p$ directions one obtains the original form of the Wilkins [1] slide line force model that is commonly cited. We prefer the above form since the contact forces $\vec{g}_p$ have physical significance; this also makes keeping track of the total work tally trivial.

The construction of the normal contact force for the case where points on either side of the slide line are no longer coincident, as depicted in Fig. 1, is as follows: for the lower side, $\vec{g}_{l,p}$, all upper side variables are rescaled by the factor $a_{l,p}/a_{u,p'}$, where the a's are the magnitudes of the area vectors used to construct the respective $\hat{c}$'s, and where p' denotes the point on the upper side that is nearest to point "p" on the lower side. Since we are only interested in the force normal to the slide line we perform a rotation of this normal component simply by letting $\vec{F}_{u,p'} \cdot \hat{c}_{l,p} \to -\vec{F}_{u,p'} \cdot \hat{c}_{u,p'}$. (Wilkins rotates the total stress on the upper side and then projects in the $\hat{c}_{l,p}$ direction; the above is equivalent but much easier to implement! The minus sign occurs because the $\hat{c}$'s are defined as respective outward normals.) The final result is

$$\vec{g}_{l,p} \to (\vec{g}_{l,p} \cdot \hat{c}_{l,p})\hat{c}_{l,p} = -\frac{(M_{l,p}\vec{F}_{u,p'} \cdot \hat{c}_{u,p'} + M_{u,p'}\vec{F}_{l,p} \cdot \hat{c}_{l,p})a_{l,p}\hat{c}_{l,p}}{(a_{l,p}M_{u,p'} + a_{u,p'}M_{l,p})}, \tag{0.4}$$

which is what is coded.

If velocity is advanced in time along a slide line using the contact forces Eq. (0.4) between the two sides interpenetration of points from one side into the other side will occur. This is a purely kinematical difficulty that is unrelated to the force decomposition step as can be seen from the following thought problem: suppose a slide line in the "y" direction has points with velocity $v_x(y, t^n)$ that is continuous at time t^n, then because of the "y" dependence of v_x, on the next timestep t^{n+1} for

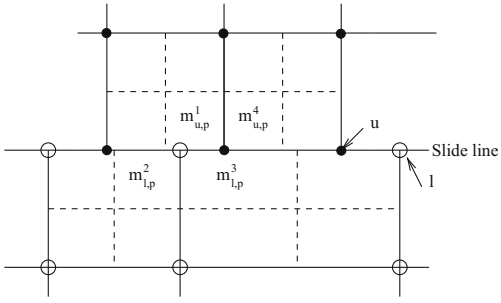

Fig. 1. Zones about a slide line where the points on the upper side "u" (solid dots), and the lower side "l" (open dots) are displaced. Corner masses $m_p^z = m_z^p$ are shown.

any amount of slide velocity v_y, $v_x(y,t^{n+1})$ will be discontinuous and interpenetration will occur. To prevent this requires additional forces that augment the contact forces. These forces of constraint are like those implicitly specified at a reflective boundary with a fixed normal $\hat{c}$, and where the boundary condition applied after the velocity advance is simply $\vec{v}_p^{n+1} \to \vec{v}_p^{n+1} - (\vec{v}_p^{n+1} \cdot \hat{c})\hat{c}$; this operation implies forces of constraint that are never calculated, and for a fixed boundary do no work. But tangential motion due to forces along the fixed boundary occur as with slide lines.

What is seen is that the boundary conditions applied to Eq. (0.1) are simply forces that can be specified in at most two ways: directly as with the contact force terms, or indirectly by specifying a component of the updated velocity. This completes a part of the right or left hand side of Eq. (0.1). If one gives the total point velocity as a function of time (as at the boundary of a driving piston) then any external force specification is simply nullified. But if only a component of the velocity is specified then a force component can complement it; this is the slide line case. One can specify $\vec{r}(t)$ at a boundary only if it can be differentiated to obtain a $\vec{v}(t)$. Since $\vec{v} = d\vec{r}/dt$, the initial condition $\vec{r}(t=0)$ over the initial spatial domain is all that is needed. This is why the usual put-back-on step cannot be viewed as a boundary condition. It can be viewed as a "reinitialization" of variables along the slide line on every timestep. These variables are then not generally dynamically connected.

The solution to the interpenetration problem as a velocity boundary condition that augments the contact force is found from the following thought problem: suppose we have a situation along a slide line where no slide occurs. This can happen because we use Eq. (0.3) in the force Eq. (0.2), or because there are no gradients along the slide line direction, and with zero initial velocity the contact forces only cause motion in the normal "x" direction. Then whatever velocity boundary condition is applied it must be null to this motion that by itself is correct. If we consider the "u" side as the "master" and the "l" side as the "slave" we must require that the displacement in the normal direction of the "l" side equal that of the master (and thus unchanged) "u" side. This gives

$$(\Delta\vec{r}_{l,p} \cdot \hat{c}_{u,p'})\hat{c}_{u,p'} = (\Delta\vec{r}^{\dagger}_{u,p'} \cdot \hat{c}_{u,p'})\hat{c}_{u,p'}. \tag{0.5}$$

In this equation $\Delta\vec{r}^{\dagger}_{u,p'} \equiv (\vec{v}^{n+1\dagger}_{u,p'} + \vec{v}^{n}_{u,p'})\Delta t/2$ and $\Delta\vec{r}_{l,p} \equiv (\vec{v}^{n+1}_{l,p} + \vec{v}^{n}_{l,p})\Delta t/2$ where the superscript "†" denotes a velocity that results from the advance in time of the force equation with contact forces included, and $\vec{v}^{n+1}_{l,p}$ is the final advanced velocity of points on the slave side. Thus in terms of velocity only we modify $\vec{v}^{n+1\dagger}_{l,p}$ by subtracting off its component in the $\hat{c}_{u,p'}$ direction and adding the new component in this direction obtained from Eq. (0.5), resulting in

$$\vec{v}^{n+1}_{l,p} = \vec{v}^{n+1\dagger}_{l,p} + \left[\left(\vec{v}^{n+1\dagger}_{u,p'} + \vec{v}^{n}_{u,p'}\right) \cdot \hat{c}_{u,p'}\right]\hat{c}_{u,p'} - \left[\left(\vec{v}^{n+1\dagger}_{l,p} + \vec{v}^{n}_{l,p}\right) \cdot \hat{c}_{u,p'}\right]\hat{c}_{u,p'}, \tag{0.6}$$

where $\vec{v}^{n+1}_{u,p} = \vec{v}^{n+1\dagger}_{u,p}$ and is unchanged. The velocity constraint given by Eq. (0.6) is null to our thought problem (a useful code check) but prevents interpenetration in the presence of a slide velocity by slaving the "l" side to the "u" side. It is also the unique solution to this problem, the only arbitrariness is the interpretation of the point "p'" on the "u" side. We use the nearest neighbor point displacement in the above and in Eq. (0.4) since this is simple and makes computer issues such as "parallelization" trivial. Higher order interpolation may be needed particularly if special symmetries are involved (spinning disks for instance), but this can become complicated especially in 3D. The solution is also less sensitive to velocity, as opposed to $\vec{r}(t)$, interpolation since velocity is the derivative of the latter. Note that for points on the "u" side of a fixed boundary ($\vec{v}_{u,p'} = 0$) Eq. (0.6) yields two limits: for $\vec{v}^{n}_{l,p} = 0$ the standard reflective boundary condition, and otherwise an elastic collision—both are physical. This equation thus allows the physics of the problem to decide what type of interaction/collision takes place. It is important to note that what has been done is to match normal displacements on each timestep rather than normal coordinates as is done in the put-back-on step. This is only a somewhat weaker constraint, so if one also matches the normal velocities then the dynamical mismatch noted earlier is minimized, which is why this "device" used for so long can give respectable results.

A common criticism of the master–slave procedure is that it introduces biasing into the results when this distinction becomes blurred. In the past this has sometimes been corrected by alternating the master and slave sides on every other timestep. This can be mimicked here by using Eq. (0.6) with its equivalent form for the upper side together on every timestep but multiplying one-half times the correction terms in brackets. How well this works and how these factors might be modified depending on the problem at hand is a question for future study.

Although our discussion so far applies to any Lagrangian scheme, for considerations of energy balance it is necessary to cast this in terms of the compatible form where energy is conserved to roundoff error [2]. Here the equation for specific internal energy "e_z" defined in zones "z" has the generic form

$$M_z(e_z^{n+1} - e_z^{n}) = -\sum_p \vec{f}^{z}_{p} \cdot \Delta\vec{r}_p, \tag{0.7}$$

where M_p and M_z are given as sums over corner masses $m_z^p = m_p^z$, and $\vec{F}_p = \sum_z \vec{f}^{p}_{z}$, etc. (See [2] for a detailed discussion.) The corner force $\vec{f}^{p}_{z} = \vec{f}^{z}_{p}$ is the principal object. It can be constructed using finite volume or element [3] methods; with the latter the element support basis must not be too large so that e_z is still locally defined in every zone.

Using the force equation we can define the slide work done on a timestep $(n+1, n)$ upon a point "p" of a slide line "sl" as $\Delta W^{n+1,n}_{p,sl}$, and given by

$$\Delta W^{n+1,n}_{p,sl} = M_p[(\vec{v}_p^{n+1})^2 - (\vec{v}_p^{n})^2]/2 - \sum_z \vec{f}^{p}_{z} \cdot \Delta\vec{r}_p, \tag{0.8}$$

where $\sum_z$ is over zones of the side containing point "p". Then defining $K^n \equiv \sum_p M_p(\vec{v}_p^n)^2/2$ and $I^n \equiv \sum_z M_z e_z^n$ over all points and zones, and using Eq. (0.7) we have

$$K^{n+1} + I^{n+1} - K^n - I^n = \sum_p \sum_z \vec{f}_z^p \cdot \Delta\vec{r}_p - \sum_z \sum_p \vec{f}_p^z \cdot \Delta\vec{r}_p + \sum_p \Delta W_{p,sl}^{n+1,n}, \tag{0.9}$$

where for zero work over exterior (non-slide line) boundaries the double sums exactly cancel allowing us to sum this result in time to obtain

$$K^n + I^n = K^{n=0} + I^{n=0} + \sum_{i=1}^{n-1} W_{i,sl}, \tag{0.10}$$

where $W_{i,sl} \equiv \sum_p \Delta W_{p,sl}^{i+1,i}$. This equation represents energy balance satisfied to roundoff error as in [2]. Given this exact energy tally it makes sense to define a slide line residual error R_{sl}^n at time level "n" as

$$R_{sl}^n \equiv W_{sl}^n/(K^n + I^n), \tag{0.11}$$

where $W_{sl}^n \equiv \sum_{i=1}^n W_{i,sl}$. This is a space and time integrated error along slide line "sl" since in the absence of friction forces a slide line should ideally result in no net work. (Friction forces are model dependent and not discussed here.)

We next briefly summarize results of numerical tests of the above slide model. A problem with 100 by 50 square zones on a unit domain in the horizontal "y" direction and a half unit domain in the vertical "x" direction is considered. At the initial time $t = 0$ all velocities are zero; the lower "x" half of this domain has unit density, the upper half density is ten; the specific internal energy e_z is zero except in the first five vertical layers of zones in the lower half where $e_z = 30.0$; this sends a shock wave to the left. We utilize reflective boundary conditions about the entire domain and a $\gamma = 5/3$ ideal gas law equation of state. Subzone anti-hourglass forces with a merit factor of 1.0 are employed [2]. A slide line is introduced between the high and low density regions. We use Eqs. (0.4) and (0.6) along this slide line. (In all calculations the master side is always the higher density region.) If Eq. (0.6) is not included interpenetration of the lighter density region into the higher density one occurs very quickly.

Results using the complete slide line model are shown in Fig. 2 with the grid and velocity vectors of the top and bottom domains at time $t = 0.3$. (These regions are shown separately since they are cut from a single logically connected grid that has spurious grid lines wrt the initially collapsed line of zones.) It is seen that the set of five zones that contained all of the internal energy initially have expanded by about a factor of ≈ 6. No interpenetration of the lower into the upper one has occured. (False interpenetration due to insufficient resolution of the initial high energy region will occur!) In Fig. 3 is shown the density at the same time in the upper and lower regions. While this problem has no known solution the maximum density for a strong shock wave with $\gamma = 5/3$ is four times the initial, and this is seen to obtain. At this time $R_{sl}^n = .0025$ and remains at about this value with time. (This is about what one expects for global energy conservation when compatible Lagrangian hydro is not used on problems of this size without slide lines.) This problem is run to $t = 0.9$ after which the time-step decays greatly; multiple reflections have occured but termination is not due to slide line difficulties and no discernable

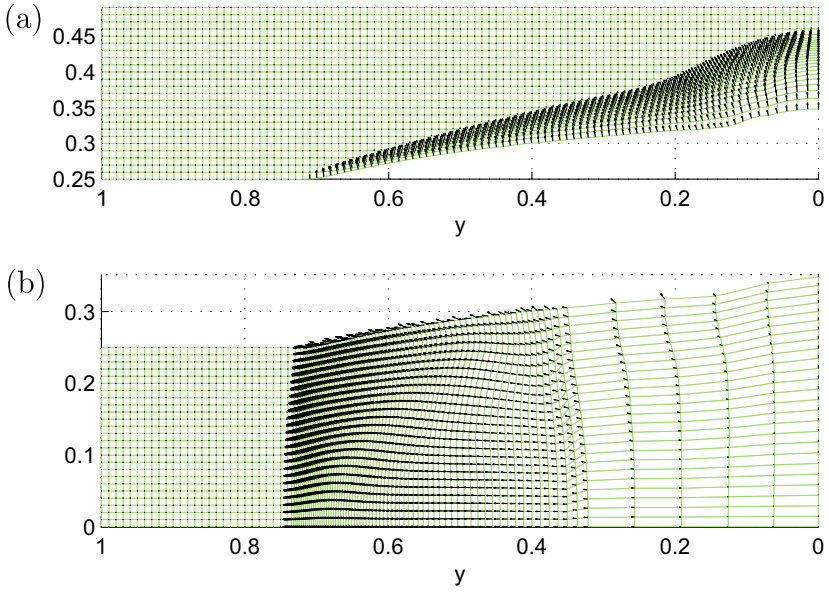

Fig. 2. Piston problem: initial $\rho = 10 : 1$, Grid and velocity vectors at $t = 0.3$ – (a) Top, "driven" high density half – (b) Bottom, low density half, first five horizontal zones are initially "hot".

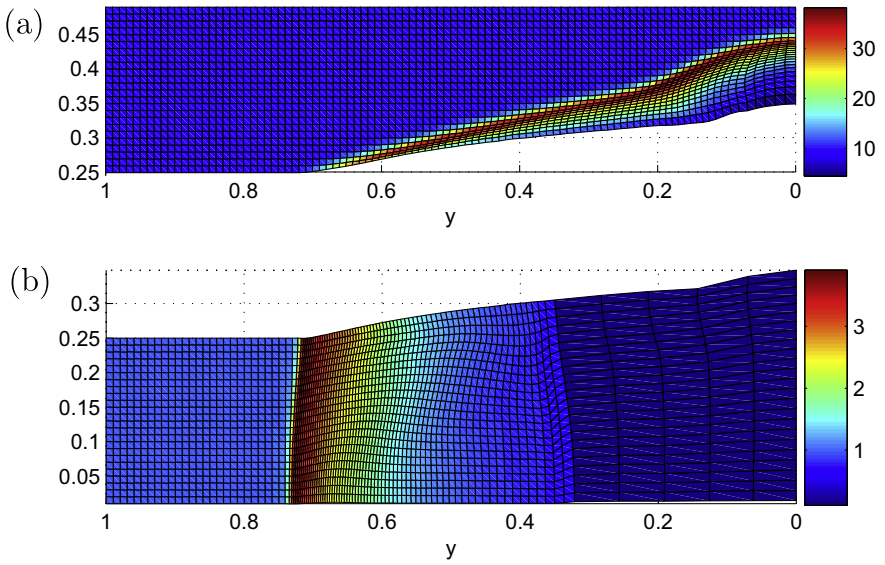

Fig. 3. Piston problem: initial $\rho = 10:1$, Density at $t = 0.3$ – (a) Top, high density half – (b) Bottom, low density half.

interpenetration is visible. Endurance is a lot of what constitutes a good slide line treatment. In this regard we have also run Raleigh–Taylor (R–T) instability problems with a slide line between the upper "heavy" and lower "light" regions. (One initializes with hydrostatic pressure balance and just perturbs the slide line/interface by a sine wave with amplitude of a small fraction of a grid spacing – 0.1 or so, and with anti-hourglass forces using a merit factor of 0.2.) While correct answers are not obtained after the linear regime this provides an endurance test where the sine wave slide velocity v_y is small compared to v_x that is normal to the interface, and where very large deformation occurs without any noticeable interpenetration. Slide lines completely rule out the possibility of Kelvin–Helmholtz instability that induces vorticity and would terminate these calculations. The "spikes" of R–T instability grow too rapidly and the "mushrooms" do not develop. Lagrangian calculations can thus fail due to grid tangling from vorticity, or they can just wipe out physical vorticity (sometimes due to anti-hourglass pressure forces) and give incorrect answers, although in the latter case some overall features and spatially integrated quantities may still be substantially correct! Anti-hourglass forces are essential to the quality of these calculations. Slide lines are sensitive to hourglass motion and one must be careful that corrections to counter this do not result in "false propagation" ahead of a shock wave.

Slide lines are most often employed when material models are used but are actually more difficult for the pure fluid problems just discussed since fluids always tend to intermix due to instability, and for cold regions the velocity dependent artificial viscosity force is all important. These forces are correct only for dynamically consistent evolving fluid states. Finally we wish to note that more complicated slide line setups, or 3D surfaces, can be readily accommodated by our new model. (The former includes "T-junctions" where two slide lines meet at a T-like intersection; here the two points at the end of the stem slide line can be held together by use of Eq. (0.3) and form one point that slides wrt the other intersected, top of the "T", slide line.)

While the discussion of boundary conditions that are proper to Newton's second law as applied to fluid elements is central to this work, we wish to note that for the staggered-spatial-grid Lagrangian model this turns out to be rather simple. (It is important to note that Eq. (0.7) requires no boundary data and is only an ODE.) Thus it appears that this Lagrangian form of the equations of fluid dynamics is more diagonal in a matrix sense than the point-centered one where boundary conditions are generally expressed in terms of the "method of characteristics", and are quite complicated even in 1D [4]. It is not clear how to connect these two descriptions, so this may result in further clarifications of this subject. (The distinction between sub and supersonic flow does not appear here even though the Lagrangian frame follows the v characteristic.)

In summary, the implementation of our slide line model consists of adding Eq. (0.4) to the rhs of the force Eq. (0.2) for all points on each side of a slide line; all velocities are then advanced in time after which Eq. (0.6) is applied to all slave slide line points. Next, other possible boundary conditions are applied to the edges of the computational domain. After this coordinates are advanced in time and Eq. (0.7) is updated along with auxiliary quantities such as grid vectors, volumes, and $\hat{c}$ terms. The above is performed twice within an overall predictor–corrector time advance [2]. At the end of each timestep the nearest neighbor list for points on a slide line is updated.

Acknowledgment

We wish to thank Dr. Ulas Ziyan for technical assistance.

References

[1] M.L. Wilkins, Calculations of elastic–plastic flow, Method Comput. Phys. 3 (1964) 211–262. also, Computer Simulation of Dynamic Phenomena, Springer-Verlag pub., 1999, (Chapter 5).
[2] A.L. Bauer, D.E. Burton, E.J. Caramana, R. Loubere, M.J. Shashkov, P.P. Whalen, The internal consistency, stability, and accuracy of the discrete, compatible formulation of Lagrangian hydrodynamics, J. Comp. Phys. 218 (2006) 572–593. and refs. therein.
[3] A.J. Barlow, A compatible finite element multi-material ALE hydrodynamics algorithm, Int. J. Num. Method Fluids 56 (2008) 953–964.
[4] C. Hirsch, Numerical Computation of Internal and External Flows, vol. 2, John Wiley & Sons Pub., 1990 (Chapters 16 and 19).